Assigning quantum labels to variationally computed rotational-vibrational eigenstates of polyatomic molecules

Edit Mátyus,[1] Csaba Fábri,[1] Tamás Szidarovszky,[1] Gábor Czakó,[1,2] Wesley D. Allen,[3] and Attila G. Császár[1,a)]

[1]*Laboratory of Molecular Spectroscopy, Institute of Chemistry, Eötvös University, P.O. Box 32, H-1518 Budapest 112, Hungary*
[2]*Department of Chemistry and Cherry L. Emerson Center for Scientific Computation, Emory University, Atlanta, Georgia 30322, USA*
[3]*Department of Chemistry and Center for Computational Chemistry, University of Georgia, Athens, Georgia 30602, USA*

A procedure is investigated for assigning physically transparent, approximate vibrational and rotational quantum labels to variationally computed eigenstates. Pure vibrational wave functions are analyzed by means of normal-mode decomposition (NMD) tables constructed from overlap integrals with respect to separable harmonic oscillator basis functions. Complementary rotational labels $J_{K_aK_c}$ are determined from rigid-rotor decomposition (RRD) tables formed by projecting rotational-vibrational wave functions ($J \neq 0$) onto products of symmetrized rigid-rotor basis functions and previously computed ($J=0$) vibrational eigenstates. Variational results for H_2O, HNCO, *trans*-HCOD, NCCO, and H_2CCO are presented to demonstrate the NMD and RRD schemes. The NMD analysis highlights several resonances at low energies that cause strong mixing and cloud the assignment of fundamental vibrations, even in such simple molecules. As the vibrational energy increases, the NMD scheme documents and quantifies the breakdown of the normal-mode model. The RRD procedure proves effective in providing unambiguous rotational assignments for the chosen test molecules up to moderate J values. © *2010 American Institute of Physics*. [doi:10.1063/1.3451075]

I. INTRODUCTION

During the past decade, remarkable progress has been achieved in the development of "numerically exact" variational methods for computing rotational-vibrational eigenstates of polyatomic molecules.[1–9] Notwithstanding the improved capabilities for converging on energy levels, the assignment and interpretation of the multitudinous resulting wave functions, especially at higher energies, remains a challenge.[10–13] The problem is often exacerbated by the use of sophisticated basis sets and coordinate representations. While an unambiguous labeling of molecular rovibrational states is helpful in the physical interpretation of measured spectra, it is required for the construction of spectroscopic databases.[14–16] Different investigations often employ different labels for the same quantum states or spectroscopic transitions, confounding efforts to compile self-consistent databases.

An ideal labeling scheme would be physically incisive and independent of the coordinates and basis functions used to represent the Hamiltonian and the wave function. However, assignment schemes can be very useful even if these requirements are not fully met. Among the techniques that have been employed in the analyses of variationally computed nuclear-motion wave functions are "node counting" along specified cuts of coordinate space,[17,18] the determination of "optimally separable" coordinates,[10,19–28] the use of natural modal representations,[18,29] and the evaluation of coordinate expectation values.[17] An alternative approach to assigning molecular eigenstates is provided by effective Hamiltonian methods, particularly in relatively low-energy regions.

The canonical models of the vibrations and rotations of a molecule are the quantum mechanical harmonic oscillator (HO) (Ref. 30) and rigid-rotor (RR) (Ref. 31) approximations, respectively. The low-lying states of semirigid molecules have traditionally been described by labels based on multidimensional normal-mode vibrational wave functions conjoined with RR rotational wave functions represented in a symmetric-top basis. A widespread preference for RRHO labels persists both for the appealing simplicity of the underlying models and for historical reasons. Of course, the RRHO labeling scheme is inherently model dependent, unlike methods based on natural modals, for example. Variational vibrational computations have often[3,32–45] employed the Eckart–Watson Hamiltonian expressed in normal coordinates,[46–48] which leads straightforwardly to a HO labeling of the lower-lying eigenstates. During the more than 30-year development of variational nuclear motion computations with exact kinetic energy operators, the emphasis has gradually shifted away from the Eckart–Watson Hamiltonian to Hamiltonians expressed in internal coordinates.[2,4–9,18,49–53] Nevertheless, for molecular systems of medium size (more than four atoms but less than eight), a special role will be

a)Electronic mail: csaszar@chem.elte.hu.

maintained for the Eckart–Watson Hamiltonian, perhaps expressed in a discrete variable representation (DVR),[54–57] using potential energy functions given in internal coordinates and a multidimensional HO basis.

This paper presents an easily automated protocol for labeling variational rovibrational wave functions by constructing certain standardized types of normal-mode decomposition (NMD) and rigid-rotor decomposition (RRD) tables. The NMD labeling scheme formalizes normal-mode representations that have long been in use for variational vibrational wave functions but have been underutilized for quantitative assignments. Our RRD approach is more novel, and it is amenable to rovibrational computations using any set of vibrational coordinates. The NMD and RRD procedures are demonstrated here by variational rovibrational computations for the H_2O, HNCO, *trans*-HCOD, NCCO, and H_2CCO molecules.

II. ROTATIONAL-VIBRATIONAL LABELING PROTOCOL

The rotational-vibrational labeling protocol leading to NMD and RRD tables was implemented in our own nuclear motion program system called DEWE.[3] DEWE employs a DVR[54,56] of the complete Eckart–Watson Hamiltonian,[46–48] a basis set composed of Hermite-DVR functions,[55,58] and a full potential energy surface (PES) expressed in arbitrary coordinates. DEWE computes the required eigenvalues and eigenfunctions iteratively.[59,60] The vibrational part of the DEWE program is described in detail in Ref. [3]. The treatment has been extended during the present work to include rotations as well.

Let us consider the n_Jth rovibrational wave function $\Psi_{n_J}^J(\mathbf{Q}, \phi, \theta, \chi)$ as a linear combination of rotational-vibrational basis functions,

$$\Psi_{n_J}^J(\mathbf{Q}, \phi, \theta, \chi) = \sum_{i=1}^{\mathcal{N}} \sum_{L=1}^{2J+1} c_{n_J, iL}^J \Phi_i(\mathbf{Q}) R_L^J(\phi, \theta, \chi), \quad (1)$$

where (ϕ, θ, χ) is the usual set of Euler angles, $\mathbf{Q} = (Q_1, Q_2, \ldots, Q_{3\mathcal{M}-6})$ denotes the normal coordinates of an $\mathcal{M}$-atomic molecule, J is the rotational quantum number, and $R_L^J(\phi, \theta, \chi)$ denotes the Wang-transformed symmetric-top rotational basis functions[31] indexed by L. The vibrational basis functions $\Phi_i(\mathbf{Q})$ are assumed to be products of one-dimensional functions in each vibrational degree of freedom, and $\mathcal{N} = N_1 N_2 \cdots N_{3\mathcal{M}-6}$ is the total size of the multidimensional vibrational basis.

A. Normal-mode decomposition of vibrations

A pure vibrational state $\psi_m(\mathbf{Q})$ ($J=0$) can be described as a linear combination of product functions of HOs,

$$\psi_m(\mathbf{Q}) = \sum_{i=1}^{\mathcal{N}} C_{m,i} \Phi_i^{HO}(\mathbf{Q}). \quad (2)$$

Due to the normalization of the wave function and the orthonormality of the basis functions, $\Sigma_{i=1}^{\mathcal{N}} |C_{m,i}|^2 = 1$ and one can write

$$C_{m,i} = \langle \Phi_i^{HO} | \psi_m \rangle_{\mathbf{Q}}. \quad (3)$$

The $|C_{m,i}|^2$ coefficients are, from now on, referred to as the elements of the NMD table.

The labeling of "exact" vibrational wave functions $\psi_m(\mathbf{Q})$ with HO quantum numbers can be accomplished by picking out the dominant contributors in Eq. (2), which can be read directly from a NMD table. This simplification is similar in spirit to that employed during potential energy distribution, kinetic energy distribution, or total energy distribution analyses[61–66] of harmonic vibrations executed within the GF formalism[30] to describe normal modes via internal coordinates.

The quantum analog[67] of the Kolmogorov–Arnold–Moser[68] theorem provides the basis for assigning quantum numbers via separability approximations, like the normal-mode model. A NMD coefficient larger than 0.5 means a close similarity of the exact, nonseparable wave function to that provided by the separable HO Hamiltonian. A smaller coefficient does not mean that no good approximate quantum numbers can be found—it simply means that the HO approximation may not provide the best separation. This study is not concerned with searching for better separations than provided by the HO approximation ubiquitous in molecular spectroscopy.

Obviously, it would be advantageous to be able to produce NMDs from arbitrary wave functions represented with arbitrary basis functions and coordinates. In general, the integral given in Eq. (3) might be computed by numerical quadratures as

$$C_{m,i} = \sum_j w_j \Phi_i^{HO}(\boldsymbol{\xi}_j) \psi_m(\boldsymbol{\xi}_j), \quad (4)$$

where w_j and $\boldsymbol{\xi}_j$ are appropriately chosen quadrature weights and points, respectively, in the multidimensional space, and real-valued functions are assumed. However, if the variational wave functions are computed by programs built upon the use of internal coordinates, the computation of NMDs is hindered considerably as the internal coordinate and the HO wave functions whose overlap must be computed are based on different ranges and volume elements. Computation of NMDs is not at all simple in this case, and singularities which might arise in the Jacobi determinant could provide further difficulties.

B. Assignment and rigid-rotor decomposition of rotations

For the eigenstates of the field-free rovibrational Hamiltonian, the J rotational quantum number is exact, while the widely used K_a and K_c labels are approximate and correspond to $|K|$ for the prolate and oblate symmetric-top limits of the RR,[31] respectively. In the present subsection a two-step algorithm based on certain nonstandard overlap integrals is proposed to match the computed rovibrational states with pure vibrational states and then generate the K_a and K_c labels.

By rearranging Eq. (1), one obtains

$$\Psi_{n_J}^J(\mathbf{Q},\phi,\theta,\chi) = \sum_{L=1}^{2J+1} R_L^J(\phi,\theta,\chi)\left(\sum_{i=1}^{\mathcal{N}} c_{n_J,iL}^J \Phi_i(\mathbf{Q})\right)$$

$$= \sum_{L=1}^{2J+1} R_L^J(\phi,\theta,\chi)\psi_{n_J L}^J(\mathbf{Q}). \quad (5)$$

From now on, $\psi_{n_J L}^J(\mathbf{Q})$ will be referred to as the Lth vibrational part of $\Psi_{n_J}^J(\mathbf{Q},\phi,\theta,\chi)$. Because the eigenfunctions of the rotational-vibrational Hamiltonian are orthonormal, the overlap of a vibration-only wave function $\psi_m(\mathbf{Q})$ and a rovibrational wave function $\Psi_{n_J}^J(\mathbf{Q},\phi,\theta,\chi)$ $(J>0)$ is always zero, and thus not useful for making assignments. A way to circumvent this problem is to introduce the overlap of the Lth vibrational part of $\Psi_{n_J}^J(\mathbf{Q},\phi,\theta,\chi)$ and the vibration-only $\psi_m(\mathbf{Q})$ as

$$\mathcal{S}_{n_J L,m}^J = \langle\psi_{n_J L}^J(\mathbf{Q})|\psi_m(\mathbf{Q})\rangle_{\mathbf{Q}}$$

$$= \sum_{i=1}^{\mathcal{N}}\sum_{j=1}^{\mathcal{N}} c_{n_J,iL}^J C_{m,j}\langle\Phi_i(\mathbf{Q})|\Phi_j(\mathbf{Q})\rangle_{\mathbf{Q}}$$

$$= \sum_{i=1}^{\mathcal{N}} c_{n_J,iL}^J C_{m,i}, \quad (6)$$

where the integration is carried out over the $3\mathcal{M}-6$ vibrational coordinates, and an orthonormal vibrational basis and real linear combination coefficients are assumed. $\mathcal{S}_{n_J L,m}^J$ provides a measure of the similarity of $\psi_{n_J L}^J(\mathbf{Q})$ and $\psi_m(\mathbf{Q})$: the larger the magnitude of $\mathcal{S}_{n_J L,m}^J$, the more similar the vibrational parts of the two functions are. The next step is to sum the absolute squares of the $\mathcal{S}_{n_J L,m}^J$ quantities with respect to L,

$$P_{n_J,m}^J = \sum_{L=1}^{2J+1} |\mathcal{S}_{n_J L,m}^J|^2 = \sum_{L=1}^{2J+1}\left|\sum_{i=1}^{\mathcal{N}} c_{n_J,iL}^J C_{m,i}\right|^2. \quad (7)$$

After converging M $J=0$ and N_J $J\neq 0$ eigenstates by variational procedures, $N_J M$ square-overlap sums are computed over all of the $J=0$ and $J\neq 0$ pairs. The quantities $P_{n_J,m}^J$ $(n_J=1,2,\ldots,N_J$ and $m=1,2,\ldots,M)$ can be regarded as elements of a rectangular matrix with N_J rows and M columns. For a given J, those $(2J+1)$ $\Psi_{n_J}^J(\mathbf{Q},\phi,\theta,\chi)$ rovibrational states belong to a selected $\psi_m(\mathbf{Q})$ pure vibrational state which give the $2J+1$ largest $P_{n_J,m}^J$ values. This means of identification is valuable because the rovibrational levels belonging to a given vibrational state appear neither consecutively nor in a predictable manner in the overall eigenspectrum.

It is important to emphasize the pronounced dependence of the quantities $P_{n_J,m}^J$ on the embedding of the body-fixed frame, as exhibited in Eqs. (5) and (7). The DEWE code employs the Eckart frame,[46] which is expected to be a trenchant choice for the overlap calculations due to a minimalized rovibrational coupling. Of course, this rotational labeling scheme can be extended to other variational rovibrational approaches employing arbitrary internal coordinates and embeddings.

After assigning $2J+1$ rovibrational levels to a pure vibrational state, the next step is to generate the K_a and K_c or

$\tau=K_a-K_c$ labels. Such assignments could be naively based on the canonical energy stacking of asymmetric-top $J_{K_a K_c}$ states, derived from the symmetric-top limits, the symmetry labels of the states, and the noncrossing rule.[31] A rigorous approach is to set up what we call RRD tables. The two approaches do not necessarily give the same labels, although this problem occurred in only one case during the present study investigating low-J states. In order to compute the RRD coefficients it is necessary to evaluate the overlap integral

$$S_{n_J,m,m_J}^J = \langle\Psi_{n_J}^J(\mathbf{Q},\phi,\theta,\chi)|\psi_m(\mathbf{Q})\cdot\varphi_{m_J}^J(\phi,\theta,\chi)\rangle_{\mathbf{Q},\phi,\theta,\chi}$$

$$= \sum_{L=1}^{2J+1}\sum_{i=1}^{\mathcal{N}} c_{n_J,iL}^J\sum_{M=1}^{2J+1}\sum_{k=1}^{\mathcal{N}} C_{m,k}\cdot\mathcal{C}_{m_J,M}^J\cdot\langle\Phi_i(\mathbf{Q})|\Phi_k(\mathbf{Q})\rangle_{\mathbf{Q}}$$

$$\cdot\langle R_L^J(\phi,\theta,\chi)|R_M^J(\phi,\theta,\chi)\rangle_{\phi,\theta,\chi}$$

$$= \sum_{L=1}^{2J+1}\sum_{i=1}^{\mathcal{N}} c_{n_J,iL}^J\cdot C_{m,i}\cdot\mathcal{C}_{m_J,L}^J \quad (8)$$

between the n_Jth rovibrational state and the product of the mth vibrational state and m_Jth RR eigenfunction. The RR component of the product is given by a linear combination of the Wang functions R_L^J with expansion coefficients $\mathcal{C}_{m_J,L}^J$,

$$\varphi_{m_J}^J(\phi,\theta,\chi) = \sum_{L=1}^{2J+1} \mathcal{C}_{m_J,L}^J R_L^J(\phi,\theta,\chi). \quad (9)$$

Note that the notation employed does not restrict the summation by symmetry; thus, certain blocks of the $\mathcal{C}_{m_J,L}^J$ coefficients will necessarily be zero. Recognizing that these coefficients are elements of a unitary matrix, the quantities in Eqs. (7) and (8) are connected by the condition

$$P_{n_J,m}^J = \sum_{m_J=1}^{2J+1} |S_{n_J,m,m_J}^J|^2. \quad (10)$$

Because the $\psi_m(\mathbf{Q})\cdot\varphi_{m_J}^J(\phi,\theta,\chi)$ functions form an orthonormal basis of dimension $\mathcal{N}(2J+1)$, it is also obvious that

$$\sum_{m=1}^{\mathcal{N}} |P_{n_J,m}^J|^2 = 1. \quad (11)$$

In light of these relationships, we define the RRD coefficients as the absolute square of the overlaps $|S_{n_J,m,m_J}^J|^2$, and arrange them in a rectangular table whose rows are the exact states under consideration, $\Psi_{n_J}^J(\mathbf{Q},\phi,\theta,\chi)$, and whose columns are the above-defined "basis" states, $\psi_m(\mathbf{Q})\varphi_{m_J}^J(\phi,\theta,\chi)$.

III. NUMERICAL EXAMPLES

After developing eigenstate labeling capabilities into our code DEWE, applicable to semirigid molecules of arbitrary size, the utility of the proposed NMD and RRD protocols was investigated for examples of three-, four-, and five-atomic molecules—H_2O, HNCO, *trans*-HCOD, NCCO, and H_2CCO. Important details of the calculations performed and definition of the normal coordinates for all the species investigated, including the appropriate transformation matrices

TABLE I. The lowest-energy part of the NMD table of $H_2{}^{16}O$.

NMD$(\nu,\omega)^{a,b}$	4715.5 ZPV (A_1)	1649.8 ω_2 (A_1)	3299.6 $2\omega_2$ (A_1)	3835.1 ω_1 (A_1)	3946.2 ω_3 (B_2)	4949.4 $3\omega_2$ (A_1)	5484.8 $\omega_1+\omega_2$ (A_1)	5596.0 $\omega_2+\omega_3$ (B_2)	6599.1 $4\omega_2$ (A_1)	7134.6 $\omega_1+2\omega_2$ (A_1)	7245.8 $2\omega_2+\omega_3$ (B_2)	7670.1 $2\omega_1$ (A_1)	7781.3 $\omega_1+\omega_3$ (B_2)	7892.4 $2\omega_3$ (A_1)		Σ
4638.3 $\psi_0(A_1)$	97	0	0	2	0	0	0	0	0	0	0	0	0	0	…	100
1595.1 $\psi_1(A_1)$	0	98	0	0	0	0	1	0	0	0	0	0	0	0	…	100
3152.2 $\psi_2(A_1)$	0	0	95	2	0	1	0	0	0	1	0	0	0	0	…	100
3657.1 $\psi_3(A_1)$	2	0	2	83	0	0	0	0	0	0	0	10	0	1	…	100
3755.7 $\psi_4(B_2)$	0	0	0	0	89	0	0	0	0	0	0	0	9	0	…	100
4667.6 $\psi_5(A_1)$	0	0	1	0	0	88	5	0	3	1	0	0	0	0	…	100
5235.5 $\psi_6(A_1)$	0	2	0	0	0	5	83	0	0	0	0	0	0	0	…	100
5331.5 $\psi_7(B_2)$	0	0	0	0	0	0	0	90	0	0	0	0	0	0	…	100
6135.1 $\psi_8(A_1)$	0	0	0	0	0	4	0	0	75	8	0	0	0	0	…	100
6776.0 $\psi_9(A_1)$	0	0	1	0	0	0	0	0	8	78	0	3	0	0	…	99
6872.2 $\psi_{10}(B_2)$	0	0	0	0	0	0	0	0	0	0	89	0	2	0	…	99
7201.2 $\psi_{11}(A_1)$	0	0	0	11	0	0	0	0	0	3	0	48	0	6	…	97
7249.2 $\psi_{12}(B_2)$	0	0	0	0	9	0	0	0	0	0	2	0	57	0	…	97
7444.9 $\psi_{13}(A_1)$	0	0	0	0	0	0	0	0	0	0	0	10	0	69	…	98
⋮	⋮	⋮	⋮	⋮	⋮	⋮	⋮	⋮	⋮	⋮	⋮	⋮	⋮	⋮		
Σ	100	100	100	99	100	100	100	100	100	100	100	98	97	98		

^{a}Rows of variational vibrational wave functions (ψ_i) with energy levels ν are decomposed in terms of columns of HO basis states with reference energy levels ω. NMD coefficients in percent; energies in cm^{-1} relative to the corresponding variational or harmonic zero-point vibrational (ZPV) level appearing in row 1 or column 1, respectively.

^{b}The decomposition was extended to 80 states in each row and column; Σ values denote the corresponding sums of the NMD coefficients over these states. Computed from the CVRQD PES of Refs. 70 and 71. Twenty basis functions were used for each vibrational degree of freedom. The nuclear masses m_H =1.007 276 5 u and $m_{^{16}O}$=15.990 526 u were adopted.

and reference structures, are given in the supplementary material.[69]

A. Normal-mode decomposition tables

1. NMD of water

Assigning the large number of computed (and measured) rovibrational states of water up to its first dissociation limit is an extremely demanding task.[17] Without valid assignments, however, there is no hope of extending the information systems characterizing water spectroscopy beyond what is available at present.[14]

Our NMD analysis of $H_2{}^{16}O$ (Table I) is based on the PES of Refs. 70 and 71. All of the vibrational eigenstates up to 7000 cm^{-1}, including the fundamentals,[72] are described accurately by the normal-mode model. The concept of polyads[12] and the polyad number P, defined here as $P=2(v_1+v_3)+v_2$, have often been used to analyze the vibrational states of water (see, e.g., Ref. 73). Large NMD coefficients ($\geq 97\%$) are found for the ground state ($P=0$) and the bending fundamental ($P=1$), both one-dimensional blocks. For the three-dimensional $P=2$ manifold ($\psi_2-\psi_4$), the strongest mixing occurs outside the polyad block; *n.b.*

$2\omega_1$ and $\omega_1+\omega_3$ contribute 10% and 9% to ψ_3 and ψ_4, respectively. This mixing would likely be diminished in a natural modal representation. Unlike the $P=2$ case, the largest mixings for the $P=3$ states ($\psi_5-\psi_7$) are found within the polyad block, in accord with the usual polyad arguments. Among the $P=4$ states ($\psi_8-\psi_{13}$), ψ_{11} is the most strongly mixed, the largest components therein being $2\omega_1(48\%)$ and $\omega_1(11\%)$. In fact, none of the diagonal NMD values for ψ_{11}, ψ_{12}, and ψ_{13} exceeds 70%, indicating that the normal-mode picture has already started to break down for the purely stretching part of the $P=4$ polyad. Thus, the NMD analysis nicely documents the anticipated transformation from normal-mode to local-mode behavior. Finally, we note that the NMD values in Table I are in full agreement with the coefficients in Eq. (33) of Whitehead and Handy,[33] despite the use of completely different PESs in the two studies. Such NMD transferability across PESs and computational methodologies is a merit for interpreting vibrational spectra.

Overall, as compared to later examples, for the low-energy states considered $H_2{}^{16}O$ provides a well-behaved example for the NMD analysis, supported also by the fact that the frequency order of the exact states corresponds to that of the harmonic basis states. For higher energies, above about

TABLE II. The lowest-energy part of the NMD table of HNCO.

$\mathrm{NMD}(\nu,\omega)^{a,b}$		4678.2 ZPV (A')	571.1 ω_5 (A')	636.0 ω_6 (A'')	814.9 ω_4 (A')	1142.2 $2\omega_5$ (A')	1207.1 $\omega_5+\omega_6$ (A'')	1272.0 $2\omega_6$ (A')	1318.3 ω_3 (A')	1386.0 $\omega_4+\omega_5$ (A')	1450.9 $\omega_4+\omega_6$ (A'')	1629.8 $2\omega_4$ (A')	1713.3 $3\omega_5$ (A')		Σ
4628.2	$\psi_0(A')$	98	0	0	0	0	0	0	0	0	0	0	0	…	99
577.2	$\psi_1(A')$	0	94	0	2	0	0	0	0	0	0	0	0	…	97
659.2	$\psi_2(A'')$	0	0	99	0	0	0	0	0	0	0	0	0	…	99
777.1	$\psi_3(A')$	0	3	0	89	0	0	0	0	1	0	2	0	…	96
1142.9	$\psi_4(A')$	0	0	0	1	80	0	6	4	1	0	0	0	…	94
1262.7	$\psi_5(A')$	0	0	0	1	2	0	27	37	22	0	0	0	…	94
1271.1	$\psi_6(A'')$	0	0	0	0	0	90	0	0	0	6	0	0	…	97
1325.1	$\psi_7(A')$	0	0	0	2	6	0	5	46	22	0	5	0	…	92
1353.9	$\psi_8(A')$	0	0	0	1	6	0	59	9	10	0	6	0	…	94
1472.9	$\psi_9(A'')$	0	0	0	0	0	7	0	0	0	88	0	0	…	97
1515.5	$\psi_{10}(A')$	0	0	0	1	0	0	2	0	30	0	49	0	…	91
1707.4	$\psi_{11}(A')$	0	0	0	0	0	0	0	0	1	0	1	69	…	89
		⋮	⋮	⋮	⋮	⋮	⋮	⋮	⋮	⋮	⋮	⋮	⋮		
	Σ	99	98	99	98	96	98	99	99	95	98	96	91		

[a]See footnote a to Table I.
[b]Obtained with an all-electron CCSD(T)/cc-pCV5Z quartic internal coordinate force field taken from Ref. 78. Seven basis functions were used for each vibrational degree of freedom. The decomposition was extended to 100 states in each row and column; Σ values denote the corresponding sums of the NMD coefficients over these states. Atomic masses, in u, $m_H = 1.007\,825$, $m_{^{14}N} = 14.003\,074$, $m_{^{12}C} = 12$, and $m_{^{16}O} = 15.994\,915$ were adopted.

12 000 cm^{-1},[17] mixing of the basis states becomes so pronounced that the normal-mode labels lose any simple physical meaning. Nevertheless, the quantitative characterization provided by the NMD array remains useful in uniquely identifying vibrational eigenstates derived from diverse sources.

2. NMD of tetra-atomic molecules

Application of the NMD procedure to three tetra-atomic test cases, HNCO, *trans*-HCOD, and NCCO, provides the arrays in Tables II–IV. Technical details related to the chosen PESs are given in supplementary material.[69] Isocyanic acid (HNCO) is a classic quasilinear molecule whose spectroscopy has been extensively studied and whose anharmonic force field was first computed by one of us in Ref. 74. The NCCO, *trans*-HCOH, and *trans*-HCOD molecules have recently been isolated and characterized for the first time, aided by selected NMD data we have previously reported.[75,76] The examples collected in this section show that strong mixing of normal-mode wave functions at low vibrational energies is not a rare exception, even for fundamentals. Interestingly, the mixing can become so strong that the very notion of a fundamental vibrational state becomes ill defined. Besides its theoretical delicacy, this behavior has practical consequences. For instance, the strong mixing is manifested in the distorted intensity pattern in the case of the $^{14}N^{13}C^{12}C^{16}O$ isotopologue (Table IV, *vide infra*).[76]

The NMD array for HNCO (Table II) includes the 12 wave functions lying below 1750 cm^{-1} in relative energy. Seven of these wave functions have leading NMD values of $\geq 80\%$. In particular, the (ν_5, ν_6, ν_4) bending fundamentals $(\psi_1 - \psi_3)$ at $(577, 659, 777)$ cm^{-1} have diagonal NMD coefficients of $(94, 99, 89)\%$, respectively, making these assignments very clear. Likewise, the $(2\nu_5, \nu_5+\nu_6, \nu_4+\nu_6)$ bending overtone and combination levels (ψ_4, ψ_6, ψ_9) at $(1143, 1271, 1473)$ cm^{-1} have diagonal NMD elements of $(80, 90, 88)\%$, in order. In stark contrast, the states (ψ_5, ψ_7, ψ_8) lying at $(1263, 1325, 1354)$ cm^{-1} involve a strong Fermi resonance triad of the $2\omega_6$, ω_3, and $\omega_4+\omega_5$ basis states. It is striking how ambiguous the identification of the ν_3 symmetric N–C–O stretching fundamental is, as the ω_3 basis state is the largest contributor to both ψ_5 and ψ_7. The best assignments for (ψ_7, ψ_8) would appear to be $(\nu_3, 2\nu_6)$, with contributions from the $(\omega_3, 2\omega_6)$ basis functions of $(46, 59)\%$, respectively. However, the only remaining possibility for $\nu_4+\nu_5$ would then become ψ_5, and the $\omega_4+\omega_5$ NMD coefficient for this wave function is only 22%, which is third largest in the list. In brief, an intricate structure is revealed for the vibrational eigenstates of HNCO in the mid-IR region that would be poorly understood without NMD as a quantitative tool.

For deuterated *trans*-hydroxymethylene *(trans*-HCOD), NMD data are reported in Table III for a total of 21 vibrational wave functions lying below 2900 cm^{-1} in relative en-

TABLE III. The lowest-energy part of the NMD table of *trans*-HCOD.

$NMD(\nu,\omega)^{a,b}$	5141.7 ZPV (A')	933.9 ω_6 (A'')	953.6 ω_5 (A')	1326.4 ω_4 (A')	1451.0 ω_3 (A')	1867.8 $2\omega_6$ (A')	1887.5 $\omega_5+\omega_6$ (A'')	1907.2 $2\omega_5$ (A')	2260.3 $\omega_4+\omega_6$ (A'')	2280.0 $\omega_4+\omega_5$ (A')	2384.9 $\omega_3+\omega_6$ (A'')	2404.6 $\omega_3+\omega_5$ (A')	2652.8 $2\omega_4$ (A')	2739.5 ω_2 (A')	2777.4 $\omega_3+\omega_4$ (A')	2801.7 $3\omega_6$ (A'')	2821.4 $\omega_5+2\omega_6$ (A')	2841.1 $2\omega_5+\omega_6$ (A'')	2860.8 $3\omega_5$ (A')	2878.9 ω_1 (A')	2902.0 $2\omega_3$ (A')		Σ
5067.4 ψ_0(A')	98	0	0	1	0	0	0	0	0	0	0	0	0	0	0	0	0	0	0	1	0	...	100
907.1 ψ_1(A'')	0	98	0	0	0	0	0	0	1	0	0	0	0	0	0	0	0	0	0	0	0	...	99
928.7 ψ_2(A')	0	0	98	0	0	0	0	0	0	1	0	0	0	0	0	0	0	0	0	0	0	...	99
1294.1 ψ_3(A')	1	0	0	92	0	0	0	0	0	0	0	0	5	0	0	0	0	0	0	0	0	...	98
1420.8 ψ_4(A')	0	0	0	0	97	0	0	0	0	0	0	0	0	0	1	0	0	0	0	0	0	...	99
1798.0 ψ_5(A')	0	0	0	0	0	90	0	5	0	0	0	0	0	1	0	0	0	0	0	1	0	...	99
1833.6 ψ_6(A'')	0	0	0	0	0	0	97	0	0	0	0	0	0	0	0	0	0	0	0	0	0	...	99
1847.1 ψ_7(A')	0	0	0	0	0	5	0	90	0	0	0	0	0	1	0	0	0	0	0	0	0	...	98
2192.5 ψ_8(A'')	0	1	0	0	0	0	0	0	91	0	0	0	0	0	0	0	0	0	0	0	0	...	99
2215.3 ψ_9(A')	0	0	1	0	0	0	0	0	0	91	0	0	0	0	0	0	0	0	0	0	0	...	98
2328.5 ψ_{10}(A'')	0	0	0	0	0	0	0	0	0	0	97	0	0	0	0	0	0	0	0	0	0	...	99
2344.1 ψ_{11}(A')	0	0	0	0	0	0	0	0	0	0	0	95	0	0	0	0	0	0	0	1	0	...	98
2566.4 ψ_{12}(A')	0	0	0	5	0	0	0	0	0	0	0	0	78	0	0	0	0	0	0	0	0	...	83
2626.8 ψ_{13}(A')	1	0	0	0	0	1	0	2	0	0	0	0	0	83	2	0	0	0	0	2	0	...	92
2675.5 ψ_{14}(A'')	0	0	0	0	0	0	0	0	1	0	0	0	0	0	0	85	0	6	0	0	0	...	96
2682.8 ψ_{15}(A')	0	0	0	0	0	0	0	0	0	0	0	1	0	5	37	0	0	0	0	45	3	...	92
2713.4 ψ_{16}(A')	0	0	0	0	0	0	0	0	0	0	0	0	0	0	0	0	70	0	21	0	0	...	96
2729.5 ψ_{17}(A')	0	0	0	0	1	0	0	0	0	0	0	1	0	0	51	0	0	0	0	33	5	...	91
2752.1 ψ_{18}(A'')	0	0	0	0	0	0	0	0	0	0	0	0	0	0	0	7	0	88	0	0	0	...	96
2757.9 ψ_{19}(A')	0	0	0	0	0	0	0	0	0	0	0	0	0	0	0	0	25	0	68	0	0	...	95
2852.6 ψ_{20}(A')	0	0	0	0	0	0	0	0	0	0	0	0	0	0	0	0	0	0	0	7	87	...	95
	⋮	⋮	⋮	⋮	⋮	⋮	⋮	⋮	⋮	⋮	⋮	⋮	⋮	⋮	⋮	⋮	⋮	⋮	⋮	⋮	⋮		
Σ	100	99	99	98	99	99	99	99	99	98	99	98	83	92	92	96	96	96	95	90	96		

[a] See footnote a to Table I.

[b] Obtained with the all-electron CCSD(T)/cc-pCVQZ quartic internal coordinate force field taken from Ref. 75. Nine basis functions were used for each vibrational degree of freedom. The decomposition was extended to 40 states in each row and column; Σ values denote the corresponding sums of the NMD coefficients over these states. Atomic masses, in u, $m_H = 1.007\,825$, $m_D = 2.014\,102$, $m_{12\text{C}} = 12$, and $m_{16\text{O}} = 15.994\,915$ were adopted.

ergy. The first 12 wave functions, including those for the fundamental levels ν_3, ν_4, ν_5, and ν_6, have dominant diagonal NMD values ($\geq 90\%$). Thus, all vibrational states lying below 2400 cm^{-1} are remarkably well described by the normal-mode picture. In contrast, the higher vibrational states appearing in Table III show substantial mixing in the NMD array. For ψ_{13} at 2627 cm^{-1}, ω_2 contributes 83%, which is still sufficient to clearly identify this state as the ν_2 (O—D stretch) fundamental. However, in attempting to assign the remaining fundamental (ν_1), we find that ψ_{15} at 2683 cm^{-1} is 45% $\omega_1 + 37\%$ ($\omega_3 + \omega_4$), whereas ψ_{17} at 2730 cm^{-1} is 33% $\omega_1 + 51\%$ ($\omega_3 + \omega_4$). These NMD data reveal that the C—H stretching fundamental is in strong Fermi resonance with a combination level involving the H—C—O bending and C—O stretching vibrations. While the best assignment for ν_1 (C—H stretch) is 2683 cm^{-1}, one must accept that the corresponding wave function ψ_{15} contains less than 50% of this vibrational character.

The NMD results for the ^{14}N^{13}C^{12}C^{16}O isotopologue of the carbonyl cyanide radical are given in Table IV for the lowest 16 vibrational wave functions, all lying below 950 cm^{-1} in relative energy. The C≡N and C=O stretching fundamentals, $\nu_1(a') = 2170$ cm^{-1} and $\nu_2(a') = 1853$ cm^{-1}, respectively, that were computed in our earlier study,[76] lie outside the energy region considered in Table IV. Large diagonal NMD coefficients ($\geq 95\%$) allow the $\nu_5(a')$, $\nu_6(a'')$, and $\nu_4(a')$ bending fundamentals to be readily assigned to wave functions ψ_1, ψ_2, and ψ_6 at 219, 262, and 567 cm^{-1}, respectively. Nonetheless, identification of the remaining C—C stretching fundamental [$\nu_3(a')$] suffers from the same type of ambiguity seen above for HNCO and *trans*-HCOD. In particular, ψ_{10} at 777 cm^{-1} and ψ_{12} at 795 cm^{-1} exhibit a strong Fermi resonance between ω_3 and the combination level $\omega_4 + \omega_5$. The apparent C—C stretching fundamental is ψ_{12}, if assigned on the basis of the 55% ω_3 contribution. However, this choice would mean that the C—C

TABLE IV. The lowest-energy part of the NMD table of $^{14}N^{13}C^{12}C^{16}O$.

$NMD(\nu,\omega)^{a,b}$	I^c		2976.1 ZPV (A')	219.4 ω_5 (A')	261.3 ω_6 (A'')	438.8 $2\omega_5$ (A')	480.7 $\omega_5+\omega_6$ (A'')	522.6 $2\omega_6$ (A')	578.7 ω_4 (A')	658.2 $3\omega_5$ (A')	700.1 $2\omega_5+\omega_6$ (A'')	742.0 $\omega_5+2\omega_6$ (A')	783.9 $3\omega_6$ (A'')	798.1 $\omega_4+\omega_5$ (A')	812.4 ω_3 (A')	840.0 $\omega_4+\omega_6$ (A'')	877.6 $4\omega_5$ (A')	919.5 $3\omega_5+\omega_6$ (A'')		Σ
2953.7	–	$\psi_0(A')$	98	0	0	0	0	0	0	0	0	0	0	0	0	0	0	0	…	99
219.1	9.3	$\psi_1(A')$	0	96	0	0	0	0	0	0	0	0	0	0	0	0	0	0	…	97
262.3	9.7	$\psi_2(A'')$	0	0	96	0	0	0	0	0	0	0	0	0	0	0	0	0	…	97
437.1	0.0	$\psi_3(A')$	0	0	0	91	0	1	0	0	0	0	0	0	1	0	0	0	…	94
488.6	0.0	$\psi_4(A'')$	0	0	0	0	93	0	0	0	0	0	0	0	0	0	0	0	…	95
522.6	0.3	$\psi_5(A')$	0	0	0	1	0	87	1	0	0	0	0	0	2	0	0	0	…	94
567.1	1.6	$\psi_6(A')$	0	0	0	0	0	1	95	0	0	0	0	1	0	0	0	0	…	99
654.2	0.0	$\psi_7(A')$	0	0	0	0	0	0	0	83	0	1	0	0	0	0	0	0	…	89
712.6	0.0	$\psi_8(A'')$	0	0	0	0	0	0	0	0	83	0	3	0	0	0	0	0	…	90
756.3	0.0	$\psi_9(A')$	0	0	0	0	0	0	0	2	0	81	0	1	0	0	0	0	…	90
776.8	4.2	$\psi_{10}(A')$	0	0	0	0	0	0	1	0	0	1	0	53	36	0	0	0	…	97
781.3	0.0	$\psi_{11}(A'')$	0	0	0	0	0	0	0	0	4	0	73	0	0	2	0	0	…	88
795.2	14.2	$\psi_{12}(A')$	0	0	0	0	0	2	0	0	0	0	0	37	55	0	0	0	…	98
832.0	0.1	$\psi_{13}(A'')$	0	0	0	0	0	0	0	0	0	0	1	0	0	92	0	0	…	96
868.5	0.0	$\psi_{14}(A')$	0	0	0	0	0	0	0	0	0	0	0	0	0	0	73	0	…	83
935.6	0.0	$\psi_{15}(A'')$	0	0	0	0	0	0	0	0	0	0	0	0	0	0	0	71	…	84
Σ			99	98	98	95	95	94	99	90	91	90	88	97	99	97	83	85		

[a]See footnote a to Table I.

[b]Obtained with the all-electron ROCCSD(T)/cc-pCVQZ quartic internal coordinate force field taken from Refs. 76 and 77. Nine basis functions were used for each vibrational degree of freedom. The decomposition was extended to 160 states in each row and column; Σ values denote the corresponding sums of the NMD coefficients over these states. Atomic masses, in u, $m_{^{14}N}=14.003\,074$, $m_{^{13}C}=13.003\,355$, $m_{^{12}C}=12$, and $m_{^{16}O}=15.994\,915$ were adopted.

[c]Vibrational intensities corresponding to excitations from the ZPV level, $I/km\,mol^{-1}$, were obtained with the DEWE program and an AE-ROCCSD(T)/cc-pCVTZ third-order dipole field (Ref. 76).

stretch in $^{14}N^{13}C^{12}C^{16}O$ is shifted +9.1 cm^{-1} relative to the corresponding wavenumber in the parent isotopologue. In other words, a counterintuitive blueshift occurs upon substitution of a heavier carbon isotope, as discussed in Ref. 76, illustrating the intricacies that Fermi resonances can engender. The strong mixing also manifests itself in the computed "intensity stealing" between ψ_{10} and ψ_{12}, as documented in Table IV.

3. NMD of ketene

In previous years the five-atomic ketene molecule (H$_2$CCO) was too large for adequate variational nuclear motion treatments. This proved to be quite unfortunate because ketene exhibits several peculiar spectroscopic features, as summarized in Refs. 79–81. Some of the complexities in the lower end of the high-resolution rovibrational spectrum of ketene arise because the three lowest fundamentals cluster in the 430–610 cm^{-1} region and the next two fundamentals occur in the 960–1120 cm^{-1} window. Understanding the ensuing resonances, assigning their spectral signatures, and treating them with theoretical techniques encounter severe

difficulties. Thus, it is no surprise that "the rich history of infrared and microwave studies of the ketene molecule is a microcosm of the development of modern spectroscopy" (Ref. 79). The NMD and RRD tables generated in this study serve well the purpose of unraveling the complex spectroscopy of this simple molecule.

Table V presents the NMD table of ketene for vibrational states up to 1520 cm^{-1} in relative energy. The underlying variational computations are based on the local PES of Ref. 79. The vibrational states up to 1050 cm^{-1} exhibit little mixing and have dominant NMD coefficients of $\geq 91\%$. However, most of the states in the 1050–1550 cm^{-1} window have much smaller leading NMD coefficients due to anharmonic resonances. The wave functions $(\psi_8, \psi_9, \psi_{10}, \psi_{11})$ lying at $(1071, 1113, 1169, 1211)$ cm^{-1} involve a complicated $(2\omega_6, \omega_5+\omega_6, \omega_4, 2\omega_5)$ Fermi resonance tetrad that clouds the assignment of the C=C stretching fundamental (ν_4). A striking manifestation is that the $\omega_5+\omega_6$ basis state contributes between 12% and 45% to all variational wave functions in the set $(\psi_8 - \psi_{11})$. Our current NMD results differ substantially from the more approximate coefficients extracted in

TABLE V. The lowest-energy part of the NMD table of ketene (H_2CCO).

$\mathrm{NMD}(\nu,\omega)^{a,b}$	6891.5 ZPV (A_1)	433.6 ω_9 (B_2)	502.6 ω_6 (B_1)	581.9 ω_5 (B_1)	867.2 $2\omega_9$ (A_1)	936.2 $\omega_6+\omega_9$ (A_2)	996.0 ω_8 (B_2)	1005.2 $2\omega_6$ (A_1)	1015.5 $\omega_5+\omega_9$ (A_2)	1084.5 $\omega_5+\omega_6$ (A_1)	1146.0 ω_4 (A_1)	1163.8 $2\omega_5$ (A_1)	1300.8 $3\omega_9$ (B_2)	1369.8 $\omega_6+2\omega_9$ (B_1)	1415.2 ω_3 (A_1)	1429.6 $\omega_8+\omega_9$ (A_1)	1438.8 $2\omega_6+\omega_9$ (B_2)	1449.1 $\omega_5+2\omega_9$ (B_1)	1498.6 $\omega_6+\omega_8$ (A_2)		Σ
6832.0 $\psi_0(A_1)$	98	0	0	0	0	0	0	0	0	0	0	0	0	0	0	0	0	0	0	…	99
437.1 $\psi_1(B_2)$	0	98	0	0	0	0	0	0	0	0	0	0	0	0	0	0	0	0	0	…	98
534.0 $\psi_2(B_1)$	0	0	91	6	0	0	0	0	0	0	0	0	0	0	0	0	0	0	0	…	98
603.5 $\psi_3(B_1)$	0	0	5	91	0	0	0	0	0	0	0	0	0	0	0	0	0	0	0	…	97
873.5 $\psi_4(A_1)$	0	0	0	0	94	0	0	0	0	0	1	0	0	0	0	0	0	0	0	…	96
972.6 $\psi_5(B_2)$	0	0	0	0	0	0	97	0	0	0	0	0	0	0	0	0	0	0	0	…	98
974.9 $\psi_6(A_2)$	0	0	0	0	0	94	0	0	1	0	0	0	0	0	0	0	0	0	0	…	96
1047.1 $\psi_7(A_2)$	0	0	0	0	0	1	0	0	94	0	0	0	0	0	0	0	0	0	0	…	95
1071.1 $\psi_8(A_1)$	0	0	0	0	0	0	0	79	0	14	0	0	0	0	2	0	0	0	0	…	96
1113.2 $\psi_9(A_1)$	0	0	0	0	1	0	0	5	0	20	61	8	0	0	0	0	0	0	0	…	96
1168.9 $\psi_{10}(A_1)$	0	0	0	0	0	0	0	4	0	45	33	10	0	0	1	0	0	0	0	…	94
1211.1 $\psi_{11}(A_1)$	0	0	0	0	0	0	0	1	0	12	0	76	0	0	0	0	0	0	0	…	90
1309.7 $\psi_{12}(B_2)$	0	0	0	0	0	0	0	0	0	0	0	0	88	0	0	0	0	0	0	…	93
1402.3 $\psi_{13}(A_1)$	0	0	0	0	0	0	0	1	0	1	0	0	0	0	43	50	0	0	0	…	95
1412.1 $\psi_{14}(B_1)$	0	0	0	0	0	0	0	0	0	0	0	0	0	90	0	0	0	0	0	…	92
1415.9 $\psi_{15}(A_1)$	0	0	0	0	0	0	0	2	0	0	0	0	0	0	50	45	0	0	0	…	96
1490.2 $\psi_{16}(B_1)$	0	0	0	0	0	0	0	0	0	0	0	0	0	0	0	0	0	90	0	…	93
1508.2 $\psi_{17}(A_2)$	0	0	0	0	0	0	0	0	0	0	0	0	0	0	0	0	0	0	93	…	96
1515.6 $\psi_{18}(B_2)$	0	0	0	0	0	0	0	0	0	0	0	0	0	0	0	0	85	0	0	…	92
⋮	⋮	⋮	⋮	⋮	⋮	⋮	⋮	⋮	⋮	⋮	⋮	⋮	⋮	⋮	⋮	⋮	⋮	⋮	⋮		
Σ	99	98	97	97	96	95	98	93	96	92	96	94	92	92	96	95	88	93	95		

Ref. 79, attesting to the intricacies of the vibrational mixing in this region. Nevertheless, both studies concur in the assignment of the experimental band[82] at 1116.0 cm^{-1} to the ν_4 fundamental. The ν_3 (CH$_2$ scissoring) fundamental is also strongly mixed, in this case due to a resonance between $(\omega_4, \omega_8+\omega_9)$ basis states, which contribute (43%, 50%) and (50%, 45%) to (ψ_{13}, ψ_{15}), respectively. Therefore, the ketene molecule provides multiple examples in which the assignment of vibrational fundamentals is blurred. A much more detailed discussion of our variational vibrational computations on ketene will be presented in a forthcoming paper.

B. Rigid-rotor decomposition tables

According to the protocol of Sec. II B, the vibrational part of a rovibrational wave function $\Psi_{n_J}^J$ can be characterized by computing the quantities $P_{n_J,m}^J$ of Eq. (7) derived from overlap integrals with pure vibrational wave functions ψ_m. In addition, a RRD of $\Psi_{n_J}^J$ is provided by the coefficients $|S_{n_J,m,m_J}^J|^2$, where S_{n_J,m,m_J}^J is the overlap defined in Eq. (8).

Tables of RRD coefficients lead directly to K_aK_c labels for asymmetric tops. Overall, our protocol for variational computations assigns $2J+1$ clearly labeled rovibrational levels to each of the pure ($J=0$) vibrational states.

In our scheme the complete rovibrational label includes the irreducible representation (irrep) Γ of the molecular symmetry (MS) group, the total rotational angular momentum quantum number (J), K_a and K_c values corresponding to the asymmetric RR, and the normal-mode vibrational quantum numbers $(v_1, v_2, \ldots, v_{3\mathcal{M}-6})$. It is worth emphasizing that the first two labels, Γ and J, are exact, as they are valid for the exact nonintegrable Hamiltonian, while the last labels, K_a, K_c, and $(v_1, v_2, \ldots, v_{3\mathcal{M}-6})$, are inexact designations arising from the approximate rovibrational Hamiltonian.

Once a corresponding pure vibrational wave function ψ_m is identified for a rovibrational wave function $\Psi_{n_J}^J$, one could attempt to make the (K_a, K_c) assignment by assuming canonical energy ordering of asymmetric-top rotational states. While this approach seems to be valid most of the time, it breaks down occasionally due to resonances. Mislabeling is

TABLE VI. Overlap quantities $P^J_{n_j,m}$ [Eqs. (7) and (10)] for making assignments of the first 56 $J=3$ rovibrational states of $H_2{}^{16}O$ by correspondence with the first eight pure vibrational ($J=0$) states.

ν_v	4638.31	6233.38	7790.50	8295.35	8394.03	9305.88	9873.80	9969.82	Rovibrational label[a]				
$\nu_{rv}{}^b$	ZPV(A_1)	$\nu_2(A_1)$	$2\nu_2(A_1)$	$\nu_1(A_1)$	$\nu_3(B_2)$	$3\nu_2(A_1)$	$\nu_1+\nu_2(A_1)$	$\nu_2+\nu_3(B_2)$	Γ	J	K_a	K_c	Vib.
4775.07	1.00	0.00	0.00	0.00	0.00	0.00	0.00	0.00	B_1	3	0	3	ZPV
4780.59	1.00	0.00	0.00	0.00	0.00	0.00	0.00	0.00	A_2	3	1	3	ZPV
4811.68	1.00	0.00	0.00	0.00	0.00	0.00	0.00	0.00	B_2	3	1	2	ZPV
4844.61	1.00	0.00	0.00	0.00	0.00	0.00	0.00	0.00	A_1	3	2	2	ZPV
4850.47	1.00	0.00	0.00	0.00	0.00	0.00	0.00	0.00	B_1	3	2	1	ZPV
4923.53	1.00	0.00	0.00	0.00	0.00	0.00	0.00	0.00	A_2	3	3	1	ZPV
4923.73	1.00	0.00	0.00	0.00	0.00	0.00	0.00	0.00	B_2	3	3	0	ZPV
6370.54	0.00	1.00	0.00	0.00	0.00	0.00	0.00	0.00	B_1	3	0	3	ν_2
6378.12	0.00	1.00	0.00	0.00	0.00	0.00	0.00	0.00	A_2	3	1	3	ν_2
6411.05	0.00	1.00	0.00	0.00	0.00	0.00	0.00	0.00	B_2	3	1	2	ν_2
6452.43	0.00	1.00	0.00	0.00	0.00	0.00	0.00	0.00	A_1	3	2	2	ν_2
6457.98	0.00	1.00	0.00	0.00	0.00	0.00	0.00	0.00	B_1	3	2	1	ν_2
6546.09	0.00	1.00	0.00	0.00	0.00	0.00	0.00	0.00	A_2	3	3	1	ν_2
6546.25	0.00	1.00	0.00	0.00	0.00	0.00	0.00	0.00	B_2	3	3	0	ν_2
7928.12	0.00	0.00	1.00	0.00	0.00	0.00	0.00	0.00	B_1	3	0	3	$2\nu_2$
7938.87	0.00	0.00	1.00	0.00	0.00	0.00	0.00	0.00	A_2	3	1	3	$2\nu_2$
7973.50	0.00	0.00	1.00	0.00	0.00	0.00	0.00	0.00	B_2	3	1	2	$2\nu_2$
8026.56	0.00	0.00	1.00	0.00	0.00	0.00	0.00	0.00	A_1	3	2	2	$2\nu_2$
8031.63	0.00	0.00	1.00	0.00	0.00	0.00	0.00	0.00	B_1	3	2	1	$2\nu_2$
8139.39	0.00	0.00	0.99	0.00	0.00	0.01	0.00	0.00	A_2	3	3	1	$2\nu_2$
8139.51	0.00	0.00	0.99	0.00	0.00	0.01	0.00	0.00	B_2	3	3	0	$2\nu_2$
8429.68	0.00	0.00	0.00	1.00	0.00	0.00	0.00	0.00	B_1	3	0	3	ν_1
8434.85	0.00	0.00	0.00	1.00	0.00	0.00	0.00	0.00	A_2	3	1	3	ν_1
8465.70	0.00	0.00	0.00	1.00	0.00	0.00	0.00	0.00	B_2	3	1	2	ν_1
8497.18	0.00	0.00	0.00	1.00	0.00	0.00	0.00	0.00	A_1	3	2	2	ν_1
8503.07	0.00	0.00	0.00	1.00	0.00	0.00	0.00	0.00	B_1	3	2	1	ν_1
8528.94	0.00	0.00	0.00	0.00	1.00	0.00	0.00	0.00	A_2	3	0	3	ν_3
8533.70	0.00	0.00	0.00	0.00	1.00	0.00	0.00	0.00	B_1	3	1	3	ν_3
8564.97	0.00	0.00	0.00	0.00	1.00	0.00	0.00	0.00	A_1	3	1	2	ν_3
8573.52	0.00	0.00	0.00	0.99	0.01	0.00	0.00	0.00	A_2	3	3	1	ν_1
8573.65	0.00	0.00	0.00	0.99	0.01	0.00	0.00	0.00	B_2	3	3	0	ν_1
8594.78	0.00	0.00	0.00	0.01	0.99	0.00	0.00	0.00	B_2	3	2	2	ν_3
8601.03	0.00	0.00	0.00	0.01	0.99	0.00	0.00	0.00	A_2	3	2	1	ν_3
8668.18	0.00	0.00	0.00	0.00	1.00	0.00	0.00	0.00	B_1	3	3	1	ν_3
8668.42	0.00	0.00	0.00	0.00	1.00	0.00	0.00	0.00	A_1	3	3	0	ν_3
9444.01	0.00	0.00	0.00	0.00	0.00	1.00	0.00	0.00	B_1	3	0	3	$3\nu_2$
9459.85	0.00	0.00	0.00	0.00	0.00	1.00	0.00	0.00	A_2	3	1	3	$3\nu_2$
9496.01	0.00	0.00	0.00	0.00	0.00	1.00	0.00	0.00	B_2	3	1	2	$3\nu_2$
9565.94	0.00	0.00	0.00	0.00	0.00	0.99	0.00	0.00	A_1	3	2	2	$3\nu_2$
9570.36	0.00	0.00	0.00	0.00	0.00	1.00	0.00	0.00	B_1	3	2	1	$3\nu_2$
9704.43	0.00	0.00	0.01	0.00	0.00	0.98	0.00	0.00	A_2	3	3	1	$3\nu_2$
9704.53	0.00	0.00	0.01	0.00	0.00	0.98	0.00	0.00	B_2	3	3	0	$3\nu_2$
10 008.52	0.00	0.00	0.00	0.00	0.00	0.00	1.00	0.00	B_1	3	0	3	$\nu_1+\nu_2$
10 015.61	0.00	0.00	0.00	0.00	0.00	0.00	1.00	0.00	A_2	3	1	3	$\nu_1+\nu_2$
10 048.38	0.00	0.00	0.00	0.00	0.00	0.00	1.00	0.00	B_2	3	1	2	$\nu_1+\nu_2$
10 087.85	0.00	0.00	0.00	0.00	0.00	0.00	1.00	0.00	A_1	3	2	2	$\nu_1+\nu_2$
10 093.42	0.00	0.00	0.00	0.00	0.00	0.00	0.99	0.01	B_1	3	2	1	$\nu_1+\nu_2$
10 105.19	0.00	0.00	0.00	0.00	0.00	0.00	0.00	1.00	A_2	3	0	3	$\nu_2+\nu_3$
10 111.70	0.00	0.00	0.00	0.00	0.00	0.00	0.01	0.99	B_1	3	1	3	$\nu_2+\nu_3$
10 144.87	0.00	0.00	0.00	0.00	0.00	0.00	0.00	1.00	A_1	3	1	2	$\nu_2+\nu_3$
10 177.56	0.00	0.00	0.00	0.00	0.00	0.00	0.79	0.20	B_2	3	3	0	$\nu_1+\nu_2$
10 178.05	0.00	0.00	0.00	0.00	0.00	0.00	0.96	0.04	A_2	3	3	1	$\nu_1+\nu_2$
10 182.84	0.00	0.00	0.00	0.00	0.00	0.00	0.20	0.80	B_2	3	2	2	$\nu_2+\nu_3$
10 188.26	0.00	0.00	0.00	0.00	0.00	0.00	0.04	0.96	A_2	3	2	1	$\nu_2+\nu_3$
10 268.48	0.00	0.00	0.00	0.00	0.00	0.00	0.00	1.00	B_1	3	3	1	$\nu_2+\nu_3$
10 268.68	0.00	0.00	0.00	0.00	0.00	0.00	0.00	1.00	A_1	3	3	0	$\nu_2+\nu_3$

[a]Γ: Labels of the irreducible representations corresponding to the MS group $C_{2v}(M)$. J: rotational quantum number. K_a, K_c: approximate quantum numbers of the asymmetric rigid rotor. Vib.: vibrational assignment based on the NMD table. ZPV=zero-point vibrational level.

[b]Nuclear masses $m_H=1.007\ 276\ 5$ u and $m_{16_O}=15.990\ 526$ u were adopted as well as the Eckart frame specified in the supplementary material. ν_v and ν_{rv}: variational vibrational and rovibrational energy levels in cm^{-1} obtained with DEWE using 15 basis functions in each vibrational degree of freedom and the CVRQD PES of Refs. 70 and 71.

TABLE VII. Overlap quantities $P^J_{n_J,m}$ [Eqs. (7) and (10)] for making assignments of the first 28 $J=3$ rovibrational states of ketene (H_2CCO) by correspondence with the first four pure vibrational ($J=0$) states.

ν_{v}	6831.98	7269.05	7365.97	7435.49	Rovibrational label[a]				
ν_{rv}[b]	ZPV(A_1)	$\nu_9(B_2)$	$\nu_6(B_1)$	$\nu_5(B_1)$	Γ	J	K_{a}	K_{c}	Vib.
6836.02	1.00	0.00	0.00	0.00	A_2	3	0	3	ZPV
6845.13	1.00	0.00	0.00	0.00	B_1	3	1	3	ZPV
6845.21	1.00	0.00	0.00	0.00	B_2	3	1	2	ZPV
6872.58	1.00	0.00	0.00	0.00	A_2	3	2	1	ZPV
6872.58	1.00	0.00	0.00	0.00	A_1	3	2	2	ZPV
6918.25	1.00	0.00	0.00	0.00	B_1	3	3	1	ZPV
6918.25	1.00	0.00	0.00	0.00	B_2	3	3	0	ZPV
7273.11	0.00	1.00	0.00	0.00	B_1	3	0	3	ν_9
7280.30	0.00	0.98	0.01	0.00	A_2	3	1	3	ν_9
7280.38	0.00	0.98	0.01	0.00	A_1	3	1	2	ν_9
7302.34	0.00	0.94	0.04	0.02	B_1	3	2	1	ν_9
7302.34	0.00	0.94	0.04	0.02	B_2	3	2	2	ν_9
7339.80	0.00	0.89	0.08	0.03	A_2	3	3	1	ν_9
7339.80	0.00	0.89	0.08	0.03	A_1	3	3	0	ν_9
7370.01	0.00	0.00	1.00	0.00	B_2	3	0	3	ν_6
7379.84	0.00	0.01	0.99	0.00	A_1	3	1	3	ν_6
7379.91	0.00	0.01	0.99	0.00	A_2	3	1	2	ν_6
7409.11	0.00	0.04	0.95	0.01	B_2	3	2	1	ν_6
7409.11	0.00	0.04	0.95	0.01	B_1	3	2	2	ν_6
7439.54	0.00	0.00	0.00	1.00	B_2	3	0	3	ν_5
7449.46	0.00	0.01	0.00	0.99	A_1	3	1	3	ν_5
7449.54	0.00	0.01	0.00	0.99	A_2	3	1	2	ν_5
7456.88	0.00	0.06	0.90	0.02	A_2	3	3	0	ν_6
7456.88	0.00	0.06	0.90	0.02	A_1	3	3	1	ν_6
7479.44	0.00	0.02	0.00	0.98	B_2	3	2	1	ν_5
7479.44	0.00	0.02	0.00	0.98	B_1	3	2	2	ν_5
7529.42	0.00	0.05	0.01	0.94	A_1	3	3	1	ν_5
7529.43	0.00	0.05	0.01	0.94	A_2	3	3	0	ν_5

[a]Γ: Labels of the irreducible representations corresponding to the MS group $C_{2v}(M)$. J: rotational quantum number. K_{a}, K_{c}: approximate quantum numbers of the asymmetric rigid rotor. Vib.: vibrational assignment based on the NMD table. ZPV=zero-point vibrational level.

[b]Atomic masses $m_{\text{H}}=1.007\,825$ u, $m_{12_{\text{C}}}=12$ u, and $m_{16_{\text{O}}}=15.994\,915$ u were adopted as well as the Eckart frame specified in the supplementary material. ν_{v} and ν_{rv}: vibrational and rovibrational energy levels in cm^{-1} obtained with DEWE using seven and six basis functions in the bending-type and stretching-type vibrational degrees of freedom, respectively, and the quartic force field of Ref. 79.

often averted by first determining the proper irrep of the MS group for a rovibrational state and applying symmetry rules for $(K_{\text{a}}, K_{\text{c}})$ before invoking energy ordering. For example, within the ν_1 vibrational state of water, the $(K_{\text{a}}, K_{\text{c}})$ values must be [(even, even), (odd, odd), (even, odd), (odd, even)] when $\Gamma = (A_1, A_2, B_1, B_2)$, in order. In contrast, for the ν_3 vibrational state of water, the $(K_{\text{a}}, K_{\text{c}})$ values must be [(odd, even), (even, odd), (odd, odd), (even, even)] when $\Gamma = (A_1, A_2, B_1, B_2)$. These and similar rules can be built into the automatic labeling protocol. Nonetheless, RRD coefficients must be employed to establish $(K_{\text{a}}, K_{\text{c}})$ assignments more rigorously. The entries in an RRD table not only reflect the proper symmetries but also quantify the mixing of the RR functions in the exact rovibrational wave functions.

Our protocol was tested by obtaining complete rovibrational labels and constructing RRD tables for the low-lying rovibrational states of the parent isotopologues of water and ketene over several J values. Assignments based on the $P^J_{n_J,m}$ quantities are shown in Tables VI and VII for the first 56 and 28 $J=3$ states of $H_2^{16}O$ and ketene, respectively. Visual representations of our results up to $J=6$ are provided in Fig. 1 for $H_2^{16}O$, and analogous depictions for ketene are given up

to $J=3$ in Fig. 2 (the numerical values used to generate Figs. 1 and 2 are given in the supplementary material[69]). Finally, example RRD tables for manifolds of $J=6$ states of $H_2^{16}O$ and $J=3$ states of ketene are presented in Tables VIII and IX.

The need for an effective labeling protocol for rovibrational states can be readily appreciated even by a quick look at the panels of Figs. 1 and 2. The intermingling of rotational levels corresponding to different vibrational states always occurs whenever $J \geq 3$. For example, the seven $J=3$ rotational levels of $H_2^{16}O$ corresponding to the ν_1 fundamental span the 8429–8574 cm^{-1} interval, which also contains three rotational levels belonging to ν_3 that lie between 8528 and 8565 cm^{-1}. The scrambling of rovibrational states of $H_2^{16}O$ is especially evident in panels (e) and (f) of Fig. 1.

The $P^J_{n_J,m}$ diagnostics [Eqs. (7) and (10)] in Tables VI and VII are frequently very close to their ideal, unmixed values of 1.00 and are almost always greater than 0.90, thus providing unambiguous quantum labels. Nevertheless, prominent exceptions sometimes occur due to resonances, which our protocol identifies successfully. For example, Table VI reveals strong mixing between $J_{K_{\text{a}}K_{\text{c}}}$ states belonging to different combination levels of $H_2^{16}O$: the

(a) $J = 1$

(b) $J = 2$

(c) $J = 3$

(d) $J = 4$

(e) $J = 5$

(f) $J = 6$
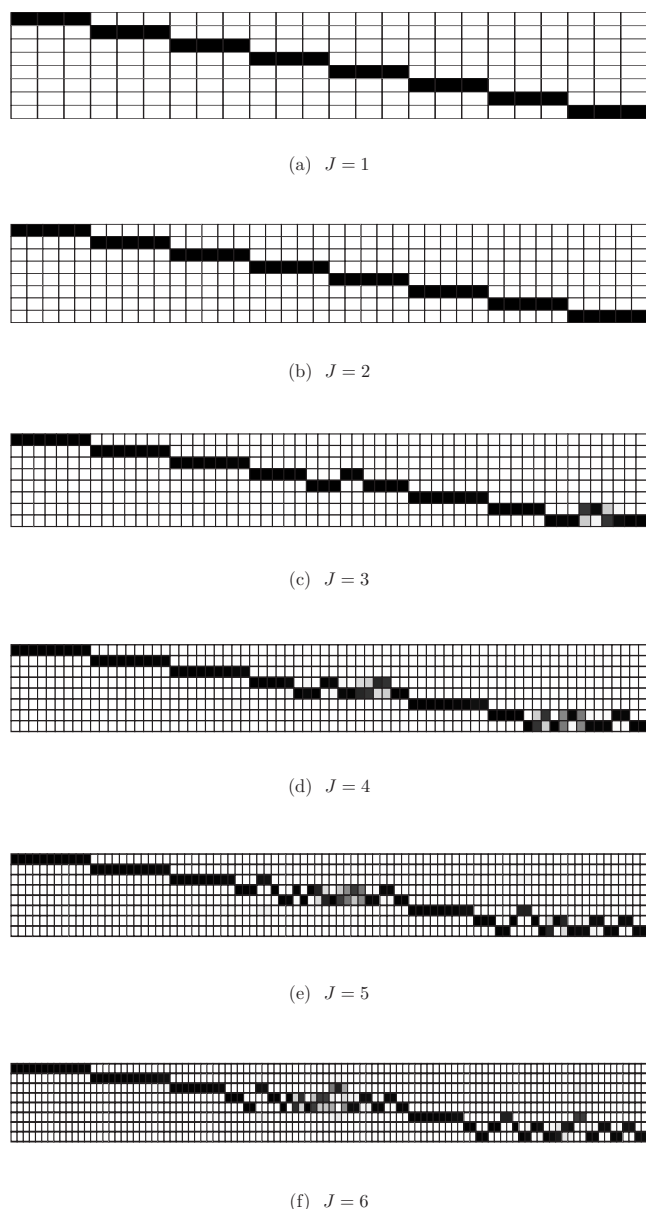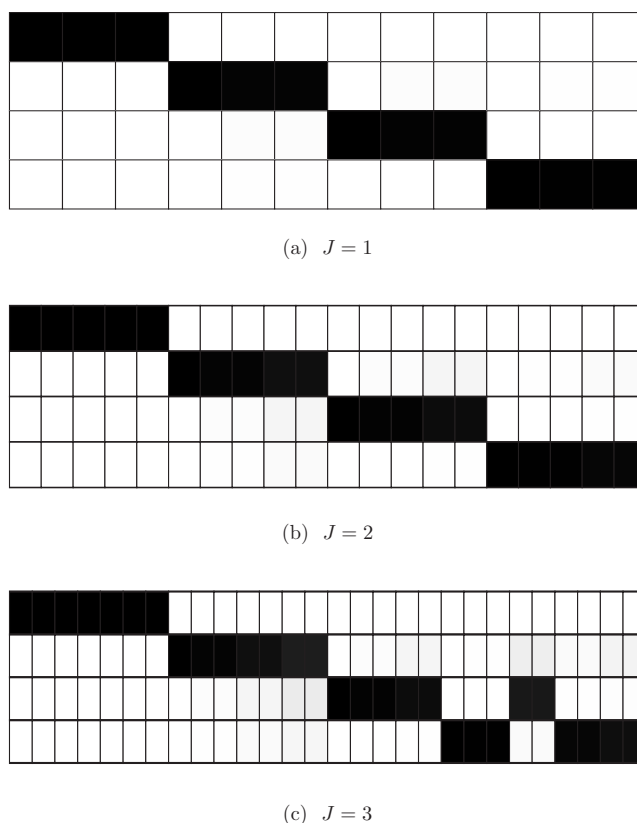
FIG. 1. Visualization of the correspondence between rovibrational states ($J>0$) and pure vibrational states ($J=0$) of $H_2{}^{16}O$, ordered in columns and rows, respectively, in terms of increasing energy. Dark squares match the $J>0$ states with their $J=0$ counterparts, according to the $P_{n_J,m}^J$ quantities in Eq. (7). The more similar the vibrational parts, the darker the square is in the figure. The variational computations utilized the DEWE code (Ref. 3), adopted the Eckart frame specified in the supplementary material (Ref. 69), and are based on the CVRQD PES (Refs. 70 and 71).

rovibrational eigenstate at 10 177.6 cm^{-1} is 79%$[3_{30}(\nu_1 + \nu_2)]$+20%$[3_{22}(\nu_2+\nu_3)]$, while that for 10 182.8 cm^{-1} is 20%$[3_{30}(\nu_1+\nu_2)]$+80%$[3_{22}(\nu_2+\nu_3)]$. This pronounced resonance causes a switching in relative energy of the 3_{30} and 3_{31} levels of $\nu_1+\nu_2$ relative to the expected RR energy ordering $[E(3_{31})<E(3_{30})]$, although the difference is less than 0.5 cm^{-1}. This case is the only one encountered for $H_2{}^{16}O$ in the current study for which the canonical sequence of RR levels is not obeyed.

Expected near degeneracies are manifested in the assignments given in Tables VI and VII. Within the bending vibrational states of water (0 υ_2 0), the $J_{J1}-J_{J0}$ rotational splitting decreases uniformly from 0.20 cm^{-1} for $\upsilon_2=0$ to

(a) $J = 1$

(b) $J = 2$

(c) $J = 3$

FIG. 2. Visualization of the correspondence between rovibrational states ($J>0$) and pure vibrational states ($J=0$) of ketene, ordered in columns and rows, respectively, in terms of increasing energy. Dark squares match the $J>0$ states with their $J=0$ counterparts, according to the $P_{n_J,m}^J$ quantities in Eq. (7). The variational computations utilized the DEWE code (Ref. 3), adopted the Eckart frame specified in the supplementary material (Ref. 69), and are based on the quartic force field of Ref. 79.

0.10 cm^{-1} for $\upsilon_2=3$, evidencing the formation of incipient local-mode pairs. The ketene molecule is very nearly a symmetric top, with (A_0, B_0, C_0) close to $(9.410, 0.343, 0.331)$ cm^{-1}, in order.[79] Accordingly, a near double degeneracy for all values of $K_a \geq 1$ is seen in the rovibrational levels in Table VII.

The RRD results in Tables VIII and IX demonstrate that the mixing among the RR wave functions is comfortably small. In all cases but one in these tables there is a dominant square-overlap coefficient of $\geq 92\%$, the exception occurring for the B_2 state of $H_2{}^{16}O$ at 7821.3 cm^{-1} that is 83%$[6_{34}(2\nu_1)]$+16%$[6_{24}(\nu_1+\nu_3)]$. The computed RRD mixing does depend slightly on the choice of rotational constants for the RR basis functions. The smallest mixing occurs if one employs the rotational constants of the corresponding pure vibrational state. Nevertheless, even if alternate choices are made, such as the equilibrium rotational constants, the increase in mixing is not sufficient to create ambiguity in the assignment protocol.

IV. SUMMARY

Powerful variational methods are increasingly used for computing accurate rovibrational states of polyatomic molecules. Standard, automated procedures are needed for assigning and interpreting the large collections of eigenstates

TABLE VIII. RRD tables, based on Eq. (8), for the $J=6$ rovibrational states of $H_2^{16}O$ corresponding to the 12th pure vibrational state, showing all contributions larger than 1%.

	$RRD(\nu_{rv}, \nu_v)^{a,b}$	ν_v	$7201.2(A_1)$	$7201.2(A_1)$	$7201.2(A_1)$	$7201.2(A_1)$	$6776.0(A_1)$	$7249.2(B_2)$	$7249.2(B_2)$	$8761.9(A_1)$
		ν_{rv}	$J_{K_aK_c}$	$6_{06}(A_1)$	$6_{24}(A_1)$	$6_{42}(A_1)$	$6_{60}(A_1)$	$6_{60}(A_1)$	$6_{34}(B_2)$	$6_{52}(B_2)$	$6_{60}(A_1)$
A_1	7631.4		100	0	0	0	0	0	0	0
	7783.7		0	99	0	0	0	1	0	0
	7927.6		0	0	94	0	0	4	1	0
	8195.5		0	0	0	95	1	0	1	1

	$RRD(\nu_{rv}, \nu_v)^{a,b}$	ν_v	$7201.2(A_1)$	$7201.2(A_1)$	$7201.2(A_1)$	$7249.2(B_2)$	$7249.2(B_2)$
		ν_{rv}	$J_{K_aK_c}$	$6_{15}(A_2)$	$6_{33}(A_2)$	$6_{51}(A_2)$	$6_{25}(B_1)$	$6_{43}(B_1)$
A_2	7725.1		99	0	0	0	0
	7838.6		0	97	0	2	1
	8049.2		0	0	97	0	3

	$RRD(\nu_{rv}, \nu_v)^{a,b}$	ν_v	$7201.2(A_1)$	$7201.2(A_1)$	$7201.2(A_1)$	$6776.0(A_1)$	$7249.2(B_2)$	$7249.2(B_2)$	$8761.9(A_1)$
		ν_{rv}	$J_{K_aK_c}$	$6_{25}(B_1)$	$6_{43}(B_1)$	$6_{61}(B_1)$	$6_{61}(B_1)$	$6_{33}(A_2)$	$6_{51}(A_2)$	$6_{61}(B_1)$
B_1	7733.0		99	0	0	0	0	0	0
	7926.7		0	92	0	0	6	1	0
	8195.5		0	0	95	1	0	1	1

	$RRD(\nu_{rv}, \nu_v)^{a,b}$	ν_v	$7201.2(A_1)$	$7201.2(A_1)$	$7201.2(A_1)$	$7249.2(B_2)$	$7249.2(B_2)$	$7444.9(A_1)$
		ν_{rv}	$J_{K_aK_c}$	$6_{16}(B_2)$	$6_{34}(B_2)$	$6_{52}(B_2)$	$6_{24}(A_1)$	$6_{42}(A_1)$	$6_{34}(B_2)$
B_2	7631.8		100	0	0	0	0	0
	7821.3		0	83	0	16	0	0
	8049.0		0	0	94	0	3	1

[a]Wave functions for rovibrational levels ν_{rv}, $\Psi_{n_j}^J(\mathbf{Q}, \phi, \theta, \chi)$ are decomposed in terms of columns of RR rotational eigenfunctions $[J_{K_aK_c}, \varphi_{m_j}^J(\phi, \theta, \chi)]$ attached to the pure vibrational states, $\psi_m(\mathbf{Q})$, lying at ν_v. RRD coefficients in percent, rounded to the nearest integer; energies in cm^{-1} relative to the ZPV energy. A RRD array is given for each of the $C_{2v}(M)$ symmetry blocks (A_1, A_2, B_1, B_2).
[b]The variational rovibrational computations were performed as specified in footnote a to Table VI. The $J=6$ RR eigenfunctions were constructed from the vibrationally averaged rotational constants of the $\nu_v=7201.2$ cm^{-1} state: $A=26.3466$ cm^{-1}, $B=14.1044$ cm^{-1}, and $C=8.9108$ cm^{-1} (Ref. 83).

resulting from state-of-the-art variational computations in order to solve chemical problems and to compile self-consistent spectroscopic databases, *inter alia.*

In this paper we demonstrate the use of NMD tables as a standard protocol for making quantitative assignments of exact, anharmonic vibrational states. Such tables follow naturally in variational approaches based on the Eckart–Watson Hamiltonian, and they are applicable, in principle, to general coordinate representations of the vibrational problem. Indeed, NMD tables can be most beneficial when coordinate systems are employed that are not chemically motivated.

A formalism for assigning rotational quantum labels to variational eigenstates with $J>0$ is needed to complement the NMD approach for $J=0$ states. We have proposed a method that uses a diagnostic evaluated from sums of squares of overlap integrals to match each rovibrational level with a pure vibrational state. After these identifications are made, RRD tables are utilized to find correspondences with asymmetric-top rotational eigenfunctions, and hence to ascribe labels. Our RRD protocol is applicable regardless of whether the vibrational part of the wave function is described well by normal-mode wave functions, and it is also able to clearly identify resonances between different rotational levels of different vibrational states.

As tests of our procedures for labeling and analyzing rovibrational eigenstates, variational computations were performed on several carefully selected molecules, namely, $H_2^{16}O$, HNCO, *trans*-HCOD, $^{14}N^{13}C^{12}C^{16}O$, and ketene (H_2CCO). The NMD and RRD protocols were implemented in the DEWE program package[3] employing the Eckart frame and normal coordinates corresponding to the actual PES used.

An interesting conclusion of the numerical results obtained is that the normal-mode picture of the vibrational bands commonly breaks down even for some of the fundamentals of molecules. Considerable mixing among some of the low-energy states seems to be the rule rather than the exception for the cases studied here. This finding may also be important for Eckart–Watson Hamiltonian-based vibrational self-consistent-field (VSCF) spectroscopy (and treatments based on such VSCF *ansätze*). Along with symmetry classification, the approximate vibrational and rotational labels attached to variationally computed rotational-vibrational eigenstates provide information much needed by experimental spectroscopists. NMD and RRD tables appear to be useful also for spectroscopic perturbation theory as they give a clear indication of extensive mixings among states which could be important when setting up the effective Hamiltonians used to

TABLE IX. RRD tables, based on Eq. (8), for the $J=3$ rovibrational states of ketene (H_2CCO) corresponding to the fourth pure vibrational state, showing all contributions larger than 1%.

	RRD$(\nu_{rv}, \nu_v)^{a,b}$	ν_v	603.5(B_1)	603.5(B_1)	437.1(B_2)	437.1(B_2)	534.0(B_1)
	ν_{rv}	$J_{K_aK_c}$	$3_{13}(B_1)$	$3_{31}(B_1)$	$3_{12}(B_2)$	$3_{30}(B_2)$	$3_{31}(B_1)$
A_1	617.5		99	0	1	0	0
	697.4		0	94	0	5	1

	RRD$(\nu_{rv}, \nu_v)^{a,b}$	ν_v	603.5(B_1)	603.5(B_1)	437.1(B_2)	437.1(B_2)	534.0(B_1)
	ν_{rv}	$J_{K_aK_c}$	$3_{12}(B_2)$	$3_{30}(B_2)$	$3_{13}(B_1)$	$3_{31}(B_1)$	$3_{30}(B_2)$
A_2	617.5		99	0	1	0	0
	697.4		0	94	0	5	1

	RRD$(\nu_{rv}, \nu_v)^{a,b}$	ν_v	603.5(B_1)	437.1(B_2)
	ν_{rv}	$J_{K_aK_c}$	$3_{22}(A_1)$	$3_{21}(A_2)$
B_1	647.4		98	2

	RRD$(\nu_{rv}, \nu_v)^{a,b}$	ν_v	603.5(B_1)	603.5(B_1)	437.1(B_2)
	ν_{rv}	$J_{K_aK_c}$	$3_{03}(A_2)$	$3_{21}(A_2)$	$3_{22}(A_1)$
B_2	607.5		100	0	0
	647.4		0	98	2

[a] See footnote a to Table VIII.
[b] The variational rovibrational computations were performed as specified in footnote a to Table VII. The $J=3$ rigid rotor eigenfunctions were constructed from the following equilibrium rotational constants: $A=9.4675$ cm^{-1}, $B=0.3443$ cm^{-1}, and $C=0.3322$ cm^{-1} (Ref. 79).

interpret high-resolution spectroscopic experiments. Thus, NMD and RRD tables, resulting in complete rovibrational labels, should be routinely computed at least for semirigid molecules.

ACKNOWLEDGMENTS

[1] J. M. Bowman, T. Carrington, and H.-D. Meyer, Mol. Phys. **106**, 2145 (2008).
[2] D. Lauvergnat and A. Nauts, J. Chem. Phys. **116**, 8560 (2002).
[3] E. Mátyus, G. Czakó, B. T. Sutcliffe, and A. G. Császár, J. Chem. Phys. **127**, 084102 (2007); E. Mátyus, J. Šimunek, and A. G. Császár, *ibid.* **131**, 074106 (2009).
[4] J. Tennyson, M. A. Kostin, P. Barletta, G. J. Harris, O. L. Polyansky, J. Ramanlal, and N. F. Zobov, Comput. Phys. Commun. **163**, 85 (2004).
[5] E. Mátyus, G. Czakó, and A. G. Császár, J. Chem. Phys. **130**, 134112 (2009).
[6] I. N. Kozin, M. M. Law, J. Tennyson, and J. M. Hutson, Comput. Phys. Commun. **163**, 117 (2004).
[7] X.-G. Wang and T. Carrington, J. Chem. Phys. **121**, 2937 (2004).
[8] S. N. Yurchenko, W. Thiel, and P. Jensen, J. Mol. Spectrosc. **245**, 126 (2007).
[9] D. Luckhaus, J. Chem. Phys. **113**, 1329 (2000).
[10] C. Jung, H. S. Taylor, and M. P. Jacobson, J. Phys. Chem. A **105**, 681 (2001).
[11] C. Jung and H. S. Taylor, J. Phys. Chem. A **111**, 3047 (2007).
[12] M. E. Kellman and V. Tyng, Acc. Chem. Res. **40**, 243 (2007).
[13] S. C. Farantos, R. Schinke, H. Gua, and M. Joyeux, Chem. Rev. (Washington, D.C.) **109**, 4248 (2009).
[14] J. Tennyson, P. F. Bernath, L. R. Brown, A. Campargue, M. R. Carleer, A. G. Császár, R. R. Gamache, J. T. Hodges, A. Jenouvrier, O. V. Naumenko, O. L. Polyansky, L. S. Rothman, R. A. Toth, A. C. Vandaele, N. F. Zobov, L. Daumont, A. Z. Fazliev, T. Furtenbacher, I. F. Gordon, S. N. Mikhailenko, and S. V. Shirin, J. Quant. Spectrosc. Radiat. Transf. **110**, 573 (2009).
[15] T. Furtenbacher, A. G. Császár, and J. Tennyson, J. Mol. Spectrosc. **245**, 115 (2007).
[16] A. G. Császár, G. Czakó, T. Furtenbacher, and E. Mátyus, Annu. Rep. Comp. Chem. **3**, 155 (2007).
[17] A. G. Császár, E. Mátyus, T. Szidarovszky, L. Lodi, N. F. Zobov, S. V. Shirin, O. L. Polyansky, and J. Tennyson, J. Quant. Spectrosc. Radiat. Transf. **111**, 1043 (2010).
[18] N. E. Klepeis, A. L. L. East, A. G. Császár, W. D. Allen, T. J. Lee, and D. W. Schwenke, J. Chem. Phys. **99**, 3865 (1993).
[19] T. C. Thompson and D. G. Truhlar, J. Chem. Phys. **76**, 1790 (1982).
[20] R. Lefebvre, Int. J. Quantum Chem. **23**, 543 (1983).
[21] N. de Leon and E. J. Heller, Phys. Rev. A **30**, 5 (1984).
[22] K. Stefański and H. S. Taylor, Phys. Rev. A **31**, 2810 (1985).
[23] P. R. Fleming and J. S. Hutchinson, J. Chem. Phys. **90**, 1735 (1989).
[24] D. W. Schwenke, J. Chem. Phys. **96**, 3426 (1992).
[25] R. C. Mayrhofer and E. L. Sibert, Theor. Chim. Acta **92**, 107 (1995).
[26] J. Zúñiga, A. Bastida, and A. Requena, J. Chem. Soc., Faraday Trans. **93**, 1681 (1997).
[27] J. Zúñiga, J. A. G. Picón, A. Bastida, and A. Requena, J. Chem. Phys. **122**, 224319 (2005).
[28] R. Dawes and T. Carrington, J. Chem. Phys. **122**, 134101 (2005).
[29] S. E. Choi and J. C. Light, J. Chem. Phys. **97**, 7031 (1992).
[30] E. B. Wilson, Jr., J. C. Decius, and P. C. Cross, *Molecular Vibrations* (McGraw-Hill, New York, 1955).
[31] R. N. Zare, *Angular Momentum: Understanding Spatial Aspects in Chemistry and Physics* (Wiley-Interscience, New York, 1988).

[32] G. D. Carney, L. I. Sprandel, and C. W. Kern, Adv. Chem. Phys. **37**, 305 (1978).

[33] R. J. Whitehead and N. C. Handy, Mol. Phys. **55**, 456 (1975).

[34] J. M. Bowman, K. M. Christoffel, and F. Tobin, J. Phys. Chem. **83**, 905 (1979).

[35] K. M. Dunn, J. E. Boggs, and P. Pulay, J. Chem. Phys. **85**, 5838 (1986).

[36] K. M. Dunn, J. E. Boggs, and P. Pulay, J. Chem. Phys. **86**, 5088 (1987).

[37] D. Searles and E. von Nagy-Felsobuki, J. Chem. Phys. **95**, 1107 (1991).

[38] J. O. Jung and R. B. Gerber, J. Chem. Phys. **105**, 10332 (1996).

[39] K. Yagi, T. Taketsugu, K. Hirao, and M. S. Gordon, J. Chem. Phys. **113**, 1005 (2000).

[40] J. M. Bowman, S. Carter, and X. Huang, Int. Rev. Phys. Chem. **22**, 533 (2003).

[41] T. Yonehara, T. Yamamoto, and S. Kato, Chem. Phys. Lett. **393**, 98 (2004).

[42] G. Rauhut, J. Chem. Phys. **121**, 9313 (2004).

[43] S. Carter, J. M. Bowman, and N. C. Handy, Theor. Chem. Acc. **100**, 191 (1998).

[44] D. Searles and E. von Nagy-Felsobuki, *Ab Initio Variational Calculations of Molecular Vibration-Rotation Spectra*, Lecture Notes in Chemistry No. 61 (Springer-Verlag, Berlin, 1993).

[45] O. Christiansen, Phys. Chem. Chem. Phys. **9**, 2942 (2007).

[46] C. Eckart, Phys. Rev. **47**, 552 (1935).

[47] J. K. G. Watson, Mol. Phys. **15**, 479 (1968).

[48] J. K. G. Watson, Mol. Phys. **19**, 465 (1970).

[49] D. W. Schwenke, J. Phys. Chem. **100**, 2867 (1996).

[50] G. Czakó, T. Furtenbacher, A. G. Császár, and V. Szalay, Mol. Phys. **102**, 2411 (2004).

[51] T. Furtenbacher, G. Czakó, B. T. Sutcliffe, A. G. Császár, and V. Szalay, J. Mol. Struct. **780–781**, 283 (2006).

[52] M. Mladenović, Spectrochim. Acta, Part A **58**, 795 (2002).

[53] B. Fehrensen, D. Luckhaus, and M. Quack, Chem. Phys. Lett. **300**, 312 (1999).

[54] D. O. Harris, G. G. Engerholm, and W. D. Gwinn, J. Chem. Phys. **43**, 1515 (1965).

[55] V. Szalay, J. Chem. Phys. **99**, 1978 (1993).

[56] V. Szalay, G. Czakó, Á. Nagy, T. Furtenbacher, and A. G. Császár, J. Chem. Phys. **119**, 10512 (2003).

[57] S. E. Choi and J. C. Light, J. Chem. Phys. **92**, 2129 (1990).

[58] P. R. Bunker and P. Jensen, *Molecular Symmetry and Spectroscopy* (NRC Research Press, Ottawa, 1998).

[59] C. Lanczos, J. Res. Natl. Bur. Stand. **45**, 255 (1950).

[60] X.-G. Wang and T. Carrington, Jr., J. Chem. Phys. **114**, 1473 (2001).

[61] H. W. Woolley, J. Chem. Phys. **17**, 347 (1949).

[62] Y. Morino and K. Kuchitsu, J. Chem. Phys. **20**, 1809 (1952).

[63] W. J. Taylor, J. Chem. Phys. **23**, 1780 (1955).

[64] P. Pulay and F. Török, Acta Chir. Hung. **44**, 287 (1965).

[65] G. Keresztury and G. Jalsovszky, J. Mol. Struct. **10**, 304 (1971).

[66] W. D. Allen, A. G. Császár, and D. A. Horner, J. Am. Chem. Soc. **114**, 6834 (1992).

[67] G. Hose and H. S. Taylor, Phys. Rev. Lett. **51**, 947 (1983).

[68] V. I. Arnold, *Mathematical Methods of Classical Mechanics*, Graduate Texts in Mathematics (Springer-Verlag, New York, 1978).

[69] See supplementary material at http://dx.doi.org/10.1063/1.3451075 for the definition of the normal coordinates, the reference structures used in this study, and for numerical values used to generate Figs. 1 and 2.

[70] P. Barletta, S. V. Shirin, N. F. Zobov, O. L. Polyansky, J. Tennyson, E. F. Valeev, and A. G. Császár, J. Chem. Phys. **125**, 204307 (2006).

[71] O. L. Polyansky, A. G. Császár, S. V. Shirin, N. F. Zobov, P. Barletta, J. Tennyson, D. W. Schwenke, and P. J. Knowles, Science **299**, 539 (2003).

[72] J. Tennyson, N. F. Zobov, R. Williamson, O. L. Polyansky, and P. F. Bernath, J. Phys. Chem. Ref. Data **30**, 735 (2001).

[73] A. G. Császár and I. M. Mills, Spectrochim. Acta, Part A **53**, 1101 (1997).

[74] A. L. L. East, C. S. Johnson, and W. D. Allen, J. Chem. Phys. **98**, 1299 (1993).

[75] P. R. Schreiner, H. P. Reisenauer, F. C. Pickard, A. C. Simmonett, W. D. Allen, E. Mátyus, and A. G. Császár, Nature (London) **453**, 906 (2008).

[76] P. R. Schreiner, H. P. Reisenauer, E. Mátyus, A. G. Császár, A. Siddiqi, A. C. Simmonett, and W. D. Allen, Phys. Chem. Chem. Phys. **11**, 10385 (2009).

[77] A. C. Simmonett, F. A. Evangelista, W. D. Allen, and H. F. Schaefer, J. Chem. Phys. **127**, 014306 (2007).

[78] Y. Bing, A. C. Simmonett, G. Czakó, E. Mátyus, A. G. Császár, I. N. Kozin, and W. D. Allen (unpublished).

[79] A. L. L. East, W. D. Allen, and S. J. Klippenstein, J. Chem. Phys. **102**, 8506 (1995).

[80] M. Gruebele, J. W. C. Johns, and L. Nemes, J. Mol. Spectrosc. **198**, 376 (1999).

[81] L. Nemes, D. Luckhaus, M. Quack, and J. W. C. Johns, J. Mol. Struct. **517–518**, 217 (2000).

[82] J. L. Duncan, A. M. Ferguson, J. Harper, and K. H. Tonge, J. Mol. Spectrosc. **125**, 196 (1987).

[83] G. Czakó, E. Mátyus, and A. G. Császár, J. Phys. Chem. A **113**, 11665 (2009).